Applied Physics Letters

# Correlation between physical, electrical, and optical properties of $Cu_2ZnSnSe_4$ based solar cells

Cite as: Appl. Phys. Lett. **102**, 013902 (2013); https://doi.org/10.1063/1.4775366
Submitted: 13 November 2012 . Accepted: 20 December 2012 . Published Online: 10 January 2013

G. Brammertz, M. Buffière, Y. Mevel, Y. Ren, A. E. Zaghi, N. Lenaers, Y. Mols, C. Koeble, J. Vleugels, M. Meuris, and J. Poortmans









AIP Publishing

# Correlation between physical, electrical, and optical properties of $Cu_2ZnSnSe_4$ based solar cells

G. Brammertz,[1,a)] M. Buffière,[1,2] Y. Mevel,[1] Y. Ren,[1,3] A. E. Zaghi,[1,3] N. Lenaers,[1,3] Y. Mols,[1] C. Koeble,[4] J. Vleugels,[3] M. Meuris,[1] and J. Poortmans[1,2]
[1]*imec—partner of Solliance, Kapeldreef 75, 3001 Heverlee, Belgium*
[2]*Department of Electrical Engineering, KU Leuven, Kasteelpark Arenberg 10, 3001 Heverlee, Belgium*
[3]*Department of Metallurgy and Materials Engineering, KU Leuven, Kasteelpark Arenberg 44, 3001 Heverlee, Belgium*
[4]*Helmholtz-Zentrum Berlin für Materialien und Energie GmbH, Hahn-Meitner-Platz 1, 14109 Berlin, Germany*

(Received 13 November 2012; accepted 20 December 2012; published online 10 January 2013)

We report on the physical, electrical, and optical properties of $Cu_2ZnSnSe_4$ (CZTSe) solar cells based on an absorber layer fabricated by selenization of sputtered Cu, Zn, Sn multilayers. It is shown that the doping density as measured by drive level capacitance profiling is correlated exponentially to the Zn/Sn ratio of the CZTSe absorber as measured by energy dispersive X-ray spectroscopy. Furthermore, it is shown that the open circuit voltage of the cells, minority carrier lifetime, and peak position of the photoluminescence response of the absorber all correlate with the doping level and, therefore, with the Zn/Sn ratio measured in the absorber. © *2013 American Institute of Physics*. [http://dx.doi.org/10.1063/1.4775366]

$Cu_2ZnSnSe_4$ (CZTSe) and $Cu_2ZnSnS_4$ (CZTS) are being extensively studied as possible absorber materials for thin film photovoltaic devices.[1–6] These materials could offer an even cheaper solution to solar cell processing as compared to $Cu(In,Ga)(S,Se)_2$ (CIGS), or CdTe technologies, which are already widely adopted on the market, as they consist mainly of earth abundant elements. The fundamental properties of the materials look promising[7] and 11.1% efficient devices have already been demonstrated.[8]

The devices presented in this work were prepared by DC-sputtering of Cu, Zn, and Sn layers onto $5 \times 5$ cm$^2$ Mo-coated soda-lime glass substrates. The sputtered metal multi-layers were then annealed in a 100% $H_2Se$ environment for times varying from 5 to 30 min at temperatures ranging from 450 °C to 520 °C. In total, 12 different devices with different metal layer structures and different selenization times were fabricated and analyzed in this work. For solar cell processing, a standard procedure for CIGS based solar cells was used, consisting of KCN etch, chemical bath deposition of a thin n-type CdS buffer layer, and AC-sputtering of 120 nm of intrinsic ZnO followed by 250 nm of highly Al-doped ZnO.[9,10] Finally, a 50 nm Ni—1 $\mu$m Al finger grid pattern was evaporated through a shadow mask for top contact formation. Lateral isolation of the cells was performed by needle scribing. The current-voltage curve of the cell with the highest efficiency measured under AM1.5 G illumination is shown in Figure 1, together with a cross-section scanning electron microscopy (SEM) image of the complete solar cell layer structure. A total area efficiency of 7.5% was measured on a 0.75 cm$^2$ cell with an open circuit voltage $V_{oc}$ of 432 mV, a short circuit current density $J_{sc}$ of 30.5 mA/cm$^2$, and a fill factor of 56.8%. Typical crystal sizes as visible from the SEM image are on the order of one micrometer. More details on the fabrication process and the solar cell properties of different devices can be found in Ref. 11. All fabricated devices were measured with energy dispersive X-ray spectroscopy (EDX) in order to determine the Zn/Sn ratio and the Cu/(Zn + Sn) ratio of the absorber layer. In addition, the doping in the CZTSe layer of all devices was derived from room temperature drive level capacitance profiling (DLCP)[12] using

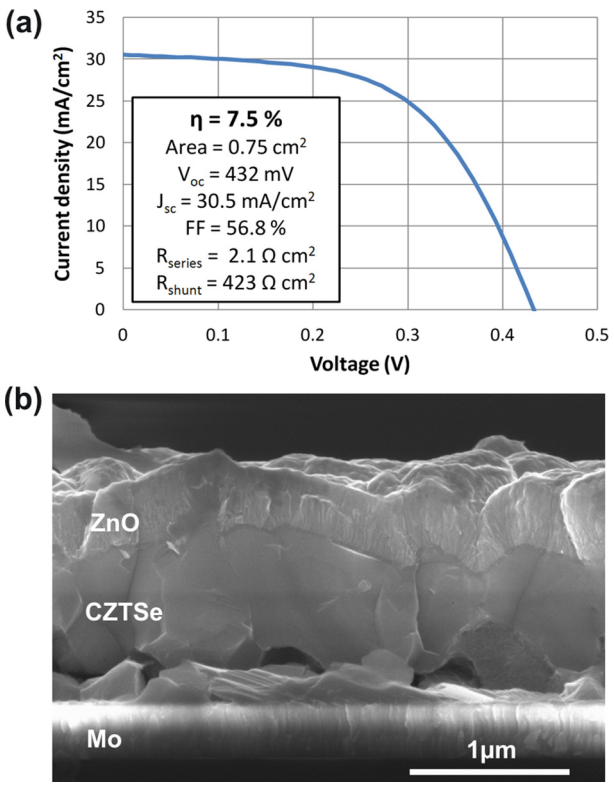


FIG. 1. Current-voltage characteristics of our highest efficiency solar cell under AM1.5 G illumination (a) and cross section SEM image of the same device (b).

[a)]Author to whom correspondence should be addressed. Electronic mail: guy.brammertz@imec.be.

 

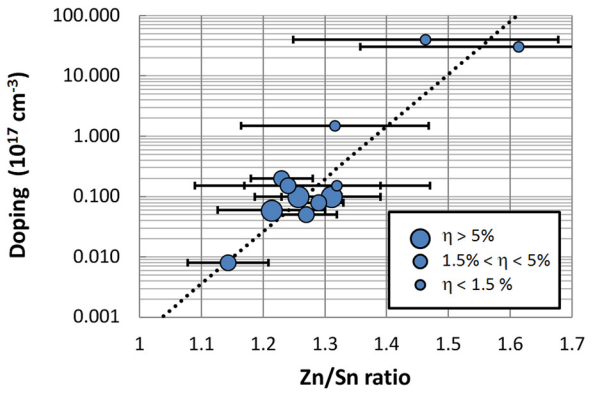


FIG. 2. Doping in the absorber as measured with DLCP as a function of the measured Zn/Sn ratio in the absorber. The properties of 12 different solar cell samples are shown. The size of the data point gives an indication of cell efficiency.

a dielectric constant value of 10. DLCP measurements were performed with an Agilent 4980 A LCR-meter with frequencies varying from 10 kHz to 100 kHz and AC voltage varying from 30 mV to 180 mV, whereas SEM and EDX analysis of the cell cross sections was made with a FEI XL-30 F tool. The operating voltage of the field emission gun for the electron beam was 15 kV, and an acquisition area corresponding to a spot size of about one micrometer of diameter was used, focused onto a CZTSe grain in the SEM cross section. Care was taken not to include the top contact CdS and ZnO layer in the EDX analysis. The average composition of three different measurement positions was determined for each sample. Figure 2 shows the doping density in the absorber layer as measured by DLCP as a function of the Zn/Sn ratio as determined from EDX of the 12 different samples. The size of the data point gives an indication of the cell efficiency of the different samples, which varies from 0.5% to 7.5%. The error bars on the Zn/Sn values show the standard deviation of the measurement values as derived from the three different measurements on the same sample. The standard deviation on the Zn/Sn ratio as a function of different positions in the sample is generally of the order of 0.05, except for the samples with Zn/Sn > 1.3, where the presence of a non-negligible amount of ZnSe secondary phases could influence the measurement results and increases the standard deviation to above 0.15. Despite the error bars on the composition measurements, a clear correlation can be identified between the Zn/Sn ratio and the doping in the absorber. The Cu/(Zn + Sn) ratio cannot be correlated with any of the electrical measurements (not shown), but it must be noted that all our cells posses a Cu/(Zn + Sn) ratio between 0.75 and 0.85, and it, therefore, varies in a relatively small range. Two possible conclusions can be drawn from these measurements. Either Zn and/or Sn are directly involved or at least very strongly influence the main defect responsible for doping in the CZTSe, or the increasing amount of Zn creates Zn based secondary phases, which increase the doping in the absorber. The exact physical nature of the doping source cannot be determined from these measurements. More precise physical analysis on the atomic scale is necessary to conclude on this. As already noted previously,[4] the highest efficiencies occur at a Zn/Sn of about 1.2, where the doping in the absorber is approximately $10^{16}$ cm$^{-3}$.

More experimental details on the doping in the CZTSe and its consequences on optical and electrical characteristics of the absorber layers and solar cells can be found on one same substrate. Figure 3(a) shows a picture of one of our $5 \times 5$ cm$^2$ samples, on which 15 different $1 \times 1$ cm$^2$ cells were fabricated. The cell in the top left corner is not a solar cell, but contains structures for physical and electrical analysis. The silver color area in the top part of the substrate is an Indium contact for better contact to the Mo backside metal, and the vertical line around the center of the sample is a breakage line where the sample was broken in two pieces for cross-section SEM analysis. We have measured the 15 different solar cells over the area of the device with illuminated

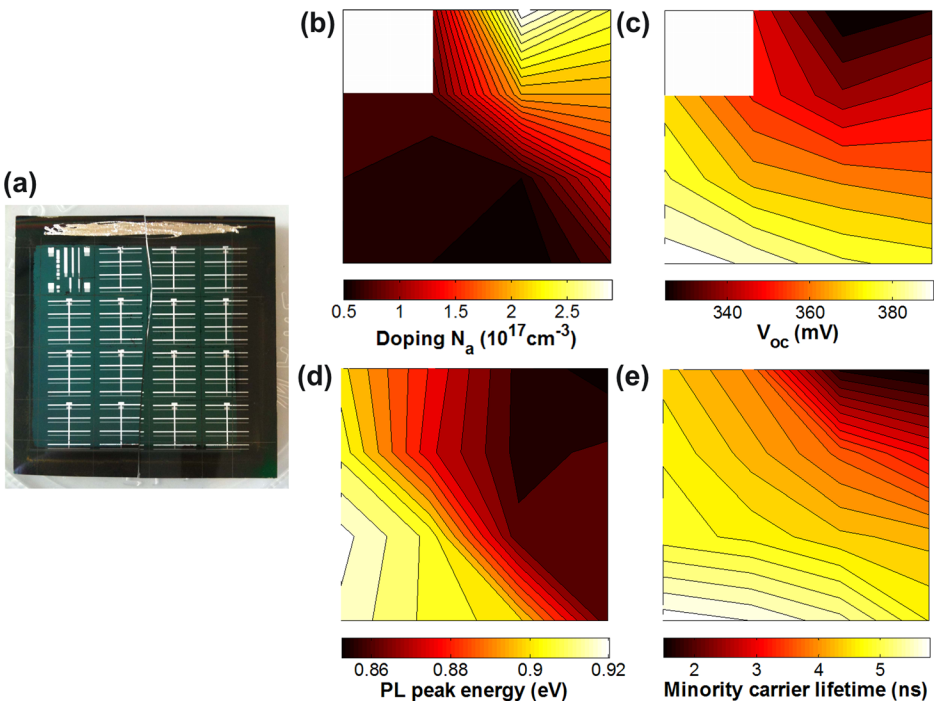


FIG. 3. Picture of the solar cell sample with 15 different cells (a), contour plot of the doping in the absorber $N_a$ as measured with DLCP (b), open circuit voltage $V_{oc}$ (c), energy position of the photoluminescence peak (d), and minority carrier lifetime (e). All values are plotted as a function of position on the sample.

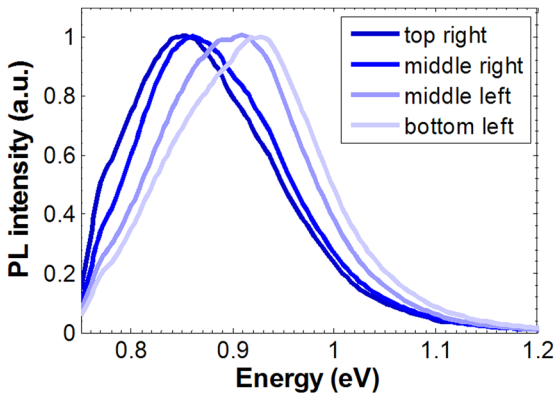


FIG. 4. Room temperature photoluminescence spectra of the solar cell sample with 15 different cells measured as a function of position. Four different spectra corresponding to four different positions along the diagonal of the sample are shown.

IV-curves, photoluminescence spectroscopy (PLS), and time resolved photoluminescence (TR-PL). PLS and TR-PL were acquired with a Hamamatsu C12132 near infrared compact fluorescence lifetime measurement system. The PLS and TR-PL measurements were made on full solar cell structures. An area of 3 mm diameter was illuminated on a solar cell with a 15 kHz, 1.2 ns pulsed 532 nm laser with 1.38 mW of average laser power. The minority carrier lifetime was derived using a two exponential fit to the photoluminescence decay curve

$$I_{PL}(t) = C_1 e^{-t/\tau_1} + C_2 e^{-t/\tau_2}, \quad (1)$$

where $I_{PL}(t)$ represents the PL intensity as a function of time. $C_1$ and $C_2$ are coefficients, $\tau_1$ and $\tau_2$ are two different decay times, with $\tau_1$ being the faster decay time and $\tau_2$ being the slower decay time. The slower decay time $\tau_2$ is assumed to be the low injection minority carrier lifetime plotted in Figure 3(e).

Figure 3(b) shows the open circuit voltage of the cells, Figure 3(c) shows the doping in the absorber as derived from DLCP measurements, Figure 3(d) shows the energy at which the PLS spectrum shows maximum intensity, and Figure 3(e) shows the minority carrier lifetime in the absorber layer. All figures show the respective values as a function of the position on the substrate. The white squares present in (b) and (c), which hide the missing data from the not present cell in the top left hand side of the sample, are not there for the optical measurement results shown in (d) and (e), because no electrical contact structure is necessary for these measurements. From the measurements, it becomes apparent that a gradient of properties exists over the area of the sample, which was due to a slight gradient of sputtered Sn thickness. We were not able to measure a difference in Zn/Sn ratio over the area of the sample, because of the relatively large errors in the SEM-EDX measurement procedure and the small relative difference in composition between the different areas of the devices. The electrical and optical measurements on the other hand are more sensitive, and a clear gradient can be identified over the area of the samples. The doping in the absorber of the different cells (Figure 3(b)) increases from the bottom left to the top right of the sample. The $V_{oc}$ of the solar cells (Figure 3(c)) and the minority carrier lifetime (Figure 3(d)) on the other hand decrease from the bottom left to the top right of the sample. Finally, the energy position of the maximum intensity in the photoluminescence response of the absorber layer also decreases from the bottom left to the top right of the sample (Figure 3(c)). In order to show more details of the photoluminescence spectra, in Figure 4, we show four different spectra corresponding to four different positions along the diagonal of the sample. The shift in energy of the photoluminescence peak can be clearly seen. The reason for the peak shift is not fully understood, but it could be that the dominant radiative recombination process in the sample goes from the conduction band to the higher energy edge of the defect level responsible for the doping. The larger this defect level will be, the broader it will become as well, and the transition can then already happen from higher energies in the defect level to the conduction band, with as a consequence a shift of the emitted photon energies towards lower values.

In summary, we have shown a correlation between the doping in CZTSe and the Zn/Sn ratio. Either Zn and/or Sn are directly involved or at least strongly influence the main defect responsible for doping in CZTSe, or the increasing amount of Zn creates Zn based secondary phases, which increase the doping in the absorber. The higher amount of doping could also be shown to influence the $V_{oc}$ of the devices, the minority carrier lifetime, and the photoluminescence peak energy.

We would like to acknowledge Tom De Geyter, Greetje Godiers, and Guido Huyberechts from Flamac in Gent for sputtering of the metal layers. AGC is acknowledged for providing substrates. The Flemish "Strategisch Initiatief Materialen" (SIM) SoPPoM program is acknowledged for their collaboration. Hamamatsu Photonics is acknowledged for providing the time resolved photoluminescence measurement system.

[1]D. B. Mitzi, O. Gunawan, T. K. Todorov, K. Wang, and S. Guha, Sol. Energy Mater. Sol. Cells **95**, 1421 (2011).
[2]A. Redinger, D. M. Berg, P. J. Dale, R. Djemour, L. Gutay, T. Eisenbarth, N. Valle, and S. Siebentritt, IEEE J. Photovolt. **1**, 200 (2011).
[3]S. Siebentritt and S. Schorr, Prog. Photovoltaics **20**, 512 (2012).
[4]S. Delbos, EPJ Photovolt. **3**, 35004 (2012).
[5]K. Ito and T. Nakazawa, Jpn. J. Appl. Phys. **27**, 2094 (1988).
[6]C. Platzer-Björkman, J. Scragg, H. Flammersberger, T. Kubart, M. Edoff, Sol. Energy Mater. Sol. Cells **98**, 110 (2012).
[7]C. Persson, J. Appl. Phys. **107**, 53710 (2010).
[8]T. K. Todorov, J. Tang, S. Bag, O. Gunawan, T. Gokmen, Y. Zhu, and D. B. Mitzi, "Beyond 11% Efficiency: Characteristics of State-of-the-Art $Cu_2ZnSn(S,Se)_4$ Solar Cells," Adv. Energy Mater. (published online).
[9]J. Klaer, I. Luck, A. Boden, R. Klenk, I. Gavilanes Perez, and R. Scheer, Thin Solid Films **431**, 534 (2003).
[10]Ch. Köble, D. Greiner, J. Klaer, R. Klenk, A. Meeder, and F. Ruske, Thin Solid Films **518**, 1204 (2009).
[11]G. Brammertz, Y. Ren, M. Buffière, S. Mertens, J. Hendrickx, H. Marko, A. E. Zaghi, N. Lenaers, C. Köble, J. Vleugels, M. Meuris, and J. Poortmans, "Electrical characterization of $Cu_2ZnSnSe_4$ solar cells from selenization of sputtered metal layers," Thin Solid Films (published online).
[12]J. T. Heath, J. D. Cohen, and W. N. Shafarman, J. Appl. Phys. **95**, 1000 (2004).